Cell, Vol. 117, 361–372, April 30, 2004, Copyright ©2004 by Cell Press

Myosin II-Dependent Cortical Movement Is Required for Centrosome Separation and Positioning during Mitotic Spindle Assembly

Jody Rosenblatt,[1,*] Louise P. Cramer,[1] Buzz Baum,[2] and Karen M. McGee[1]
[1]MRC Laboratory for Molecular Cell Biology
University College London
Gower Street
London SC1E 6BT
[2]Ludwig Institute for Cancer Research
University College London Branch
91 Riding House Street
London W1W 7BS
United Kingdom

Summary

The role of myosin II in mitosis is generally thought to be restricted to cytokinesis. We present surprising new evidence that cortical myosin II is also required for spindle assembly in cells. Drug- or RNAi-mediated disruption of myosin II in cells interferes with normal spindle assembly and positioning. Time-lapse movies reveal that these treatments block the separation and positioning of duplicated centrosomes after nuclear envelope breakdown (NEBD), thereby preventing the migration of the microtubule asters to opposite sides of chromosomes. Immobilization of cortical movement with tetravalent lectins produces similar spindle defects to myosin II disruption and suggests that myosin II activity is required within the cortex. Latex beads bound to the cell surface move in a myosin II-dependent manner in the direction of the separating asters. We propose that after NEBD, completion of centrosome separation and positioning around chromosomes depends on astral microtubule connections to a moving cell cortex.

Introduction

Microtubules and actin filaments are thought to be required for separate steps in cell division. Microtubules and microtubule motors are required for mitotic spindle formation and chromosome segregation, while actin filaments and myosin II motors are required for cytokinesis. Three lines of evidence have suggested that myosin II is needed only for cytokinesis. First, inhibition of myosin II in amphibian eggs using either anti-myosin II antibodies or myosin II fragments allows one cell division and then blocks all further divisions, but these treatments have no apparent effect on spindle formation (Meeusen et al., 1980; Kiehart et al., 1982). Second, myosin II mutations in both fission yeast and *Dictyostelium* show no mitotic defects (Bezanilla et al., 1997; de Hostos et al., 1993), and RNAi depletion of myosin II presumably only blocks cytokinesis (Somma et al., 2002). Third, mitotic spindles can form in concentrated *Xenopus* egg extracts containing high concentrations of actin depolymerising drugs (Sawin and Mitchison, 1991).

*Correspondence: jody.rosenblatt@ucl.ac.uk

Further analysis of these findings, however, questions the conclusion that myosin II is not involved in other steps of mitosis. For instance, at later time points of myosin II inhibition by antibody injection, the nuclei appeared to "fuse" together (Kiehart et al., 1982). While these nuclei may have fused after the chromosomes segregated, another possibility is that the chromosomes never initially segregated properly. More recent studies have shown that myosin II disruption after metaphase blocks anaphase as well as cytokinesis and suggest that chromosomes may also have failed to segregate in the earlier myosin II inhibition studies (Komatsu et al., 2000; Silverman-Gavrila and Forer, 2001). Whereas myosin II does not appear to be required for spindle formation in yeast and *Dictyostelium*, thorough examination of RNAi-depleted myosin II light chain (MLC) from cultured *Drosophila* cells suggests that it is important for mitosis (Somma et al., 2002). Although DNA duplicated in all cells, only half of the cells became binucleate, suggesting that the chromosomes in the other half never segregated. Furthermore, while spindle assembly in extracts has been useful in dissecting many aspects of mitosis, this cell-free system does not replicate all steps in mitosis, such as early prophase centrosomal migration along the nuclear envelope, anaphase B, and cytokinesis. One important difference from spindle assembly in a cell is that, in extracts, the spindle lacks a cell cortex and the astral microtubules that normally connect to this cortex.

Interactions of astral microtubules with the cell cortex are thought to play an important role in centering and aligning the spindle within the dividing cell. There has been intensive study of spindle alignment during asymmetric cell division, but correct spindle alignment is also important for symmetrically dividing cells. The spindle must be aligned correctly along the length of the cell so that cytokinesis occurs through the short axis or so that daughters remain in the same plane, such as in an epithelium or tissue culture. Further, spindles must be centered within a symmetrically dividing cell so that resulting daughter cells will be the same size. Moreover, because contacts between astral microtubules and the cortex are extensive during prophase, they may be important for spindle assembly as well as for correct spindle positioning within the cell.

For these reasons, we have reexamined the role of the cell cortex during spindle assembly. We find that addition of actin-depolymerizing drugs that disrupt the cell cortex (and thus the astral microtubule connections to the cortex) prevent proper spindle formation. Using improved methods to inhibit myosin II within the cortex rapidly and completely, we show that myosin II is required for normal centrosome migration and positioning around chromosomes during spindle assembly. We find that cortical myosin II activity is required for the directed movement of the cortex during spindle assembly, and, thus, attachment of the two asters to the moving cortex separates and positions them around the chromosomes during prophase. Without this activity, the spindle fails to correctly assemble and align within the cell.

Results

Actin and Myosin II Inhibitory Drugs Disrupt Spindle Assembly

To examine whether the actin/myosin-based cell cortex is required for spindle assembly, we disrupted it by depleting actin using the actin-depolymerising drug Latrunculin A. Treatment of PtK2 cells with Latrunculin A for only 20 min resulted in 48% of spindles forming aberrantly ($n = 1039$). These cells did not recover to form normal spindles while in drug, as longer treatments in Latrunculin A caused more defective spindles to accumulate (72% after 120 min where $n = 200$).

We next determined whether the actin cortex is needed for spindle assembly simply because it acts as a scaffold for astral microtubules or whether myosin II activity within the cortex was also required. To test whether myosin II is required for spindle formation, we treated PtK2 cells with drugs that specifically inactivate myosin II within 2–3 min of addition. Y-27632 inhibits Rho kinase (ROCK), which in turn blocks myosin II light chain kinase (MLCK) and thus myosin II activity. Blebbistatin specifically inhibits the ATPase of nonmuscle myosin II directly (Straight et al., 2003). We treated the cells for either 20 min or 120 min with these inhibitors (or DMSO as a control) and then fixed and immunostained them for nonmuscle myosin II, tubulin, and DNA. After 20 min in the presence of drug, 35%–50% of all spindles analyzed had defects (Figure 1D). Compared to a normal control spindle (Figure 1A), defective spindles commonly fell into two major categories: "lopsided" chromosomes that remain on one side of the asters instead of aligning between them (Figure 1B) and "at poles," in which unaligned chromosomes stay at one or both centrosomes (Figure 1C). Note that when myosin II activity is inhibited with either blebbistatin or Y-27632, astral microtubules still retain contacts with the edge of the cell (Figures 1B and 1C). In addition, occasionally monoasters or multiple asters also resulted from myosin II drug inactivation (not shown). The proportions of abnormal spindles seen after 20 and 120 min of treatment are shown in Figure 1D, with the proportions of the four types of spindle defects in Figure 1E. In addition to abnormalities in spindle morphology, approximately 19% of the defective spindles were not centered or aligned correctly within the cell. This was probably an underestimate, because most cells were not large enough or morphologically polarized enough to detect abnormal spindle positioning (see Figure 1C), but, when they were, spindle positioning was typically aberrant. These defective spindles did not recover with time, as the percentage of spindles with defects accumulated with longer drug treatments (see Figure 1E, 120′). As myosin II appears to be required for correct spindle formation, we focused on its role in spindle assembly.

Myosin II Is Required for Centrosome Separation and Positioning after NEBD

To assess the role of myosin II during spindle assembly, we studied mitotic PtK2 cells expressing EGFP-tubulin by time-lapse microscopy and disrupted myosin II activity at different times during mitosis. In control cells, there were two types of centrosomal movement. Approximately 50% of cells initiated and completed centrosome movement around the nuclear envelope prior to NEBD. In the other 50% of cells, centrosomes began movement along the nuclear envelope but completed migration by nuclear envelope-independent movement after NEBD. Nuclear envelope-dependent and -independent pathways for centrosome separation have been seen previously (Rattner and Berns, 1976; Whitehead et al., 1996). In control cells, we focused on the second movement, in which centrosomal migration initiated before and continued after NEBD. Here, the two centrosomes migrated around the nucleus as the chromosomes condensed (Figure 2A and Supplemental Movie S1 at http://www.cell.com/cgi/content/full/117/3/361/DC1). Once the nuclear envelope broke down (0:00), the asters continued to move around the chromosomes (0:31) and aligned within the cell (0:48). Soon after the chromosomes aligned at the metaphase plate, the cell underwent anaphase and then cytokinesis (at 1:20 in Supplemental Movie S1).

We discovered that myosin II activity was required for centrosome migration around the chromosomes only after NEBD. Unfortunately, we could only film cells using Y-27632, as blebbistatin rapidly photo bleached the GFP signal. However, because both inhibitors gave similar defects in the fixed-cell assay, we expect blebbistatin-mediated inhibition of myosin II would cause defects using a similar mechanism. In a cell treated with Y-27632 at time −0:05 (Figure 2B and see Supplemental Movie S2 on Cell website), the two centrosomes halted migration around the chromatin as soon as NEBD occurred (0:00), then the asters remained stuck on one side of the chromosomes (0:15), causing abnormal spindles to form with lopsided chromosomes (0:51, see Supplemental Movie S2). In this and other movies with Y-27632, the chromosomes would decondense again after 2–4 hr, even though asters remained on one side of the chromosomes, and spindle assembly never completed. Furthermore, in the Y-27632-treated movies, other events normally seen during mitosis still occur, such as cell rounding, NEBD, chromosome condensation, and decondensation, and normal microtubule dynamics-only positioning of the two asters around the chromosomes is blocked. In movies, the spindle defects that typically resulted from Y-27632 were lopsided spindles, as seen in fixed cells (Figure 1B). Sometimes, Y-27632 disruption resulted in chromosomes that became stuck at one pole, as seen in Supplemental Movie S3. Here too, centrosomes did not complete migration around the chromosomes completely. Although it is not clear why the two chromosomes did not align, a likely possibility is that when asters are not symmetrically aligned on either side of the chromosomes, the microtubules from one of the asters do not have access to all of the chromosomes. The end of Supplemental Movie S3 represents the at poles defect seen in fixed time points in Figure 1C. The at poles defects may eventually recover to form normal spindles; however, we predict that they typically do not, as long treatments of cells with Y-27632 (2 hr) resulted in a higher frequency of chromosomal nondisjunction (18% compared to 4% in DMSO-treated cells). Thus, the movies demonstrated that both of the main types of defects observed in fixed cells (lopsided and at poles)

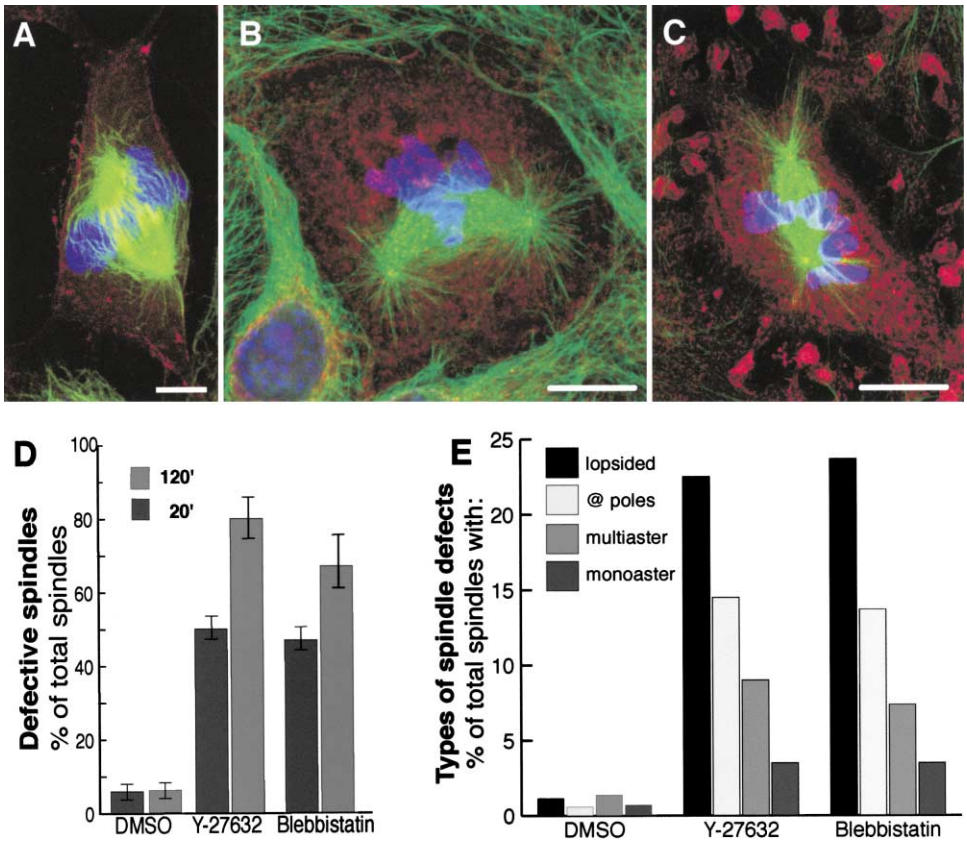

Figure 1. Drug Inhibition of Myosin II Interferes with Normal Spindle Assembly

Confocal projections of PtK2 cells treated for 20 min with 0.1% DMSO (A), 10 μM Y-27632 (B), or 100 μM blebbistatin and immunostained with α-tubulin (green) and nonmuscle myosin II antibodies (red) and with Hoechst for DNA. Percentage of abnormal spindles from each drug treatment after 20 and 120 min (D), represented as the mean (± SD) of 1,000 spindles over four experiments. In (E), the types of spindle defects are represented as the mean averaged from over 800 spindles in three experiments resulting from 20 min treatment with DMSO, Y-27632, or blebbistatin. Scale bar, 10 μm.

appeared to result from a primary defect in completion of centrosome separation and positioning.

Significantly, we found that the Y-27632-dependent spindle defects were dependent on when NEBD occurred. In six out of six movies where NEBD occurred prior to completion of centrosome separation, spindles did not form correctly, whereas, in seven out of seven movies where NEBD occurred after centrosomes had completed separation around the nuclear envelope, the spindles appeared to form normally. Figure 2C and Supplemental Movie S4 show an example of a Y-27632-treated prophase cell (−0:15) where NEBD occurred after the centrosomes had completed their migration to opposite sides of the nucleus (0:00), and spindle assembly was apparently normal (0:45). Thus, if centrosomes could position symmetrically around the chromosomes by migrating around the nuclear envelope, myosin II activity was no longer important for spindle assembly. Furthermore, while myosin II activity may contribute to centrosome movement prior to NEBD, its role does not become important until after NEBD occurs. In support of this, addition of Y-27632 had the same effect on spindle assembly, whether it was added 1 hr before NEBD or just prior to NEBD.

To determine whether myosin II activity was required for the maintenance as well as the formation of a spindle, we added Y-27632 to a preformed metaphase spindle (Figure 2D and Supplemental Movie S5). The spindle maintained normal morphology; however, it failed to enter anaphase (1:37), as documented previously (Komatsu et al., 2000). The slight shrinking of the whole spindle seen by 1:37 was due to rounding of the cell, as normally occurs during progress through mitosis. Interestingly, at low concentrations of Y-27632 (5–25 μM), spindle assembly and anaphase could be inhibited without affecting cytokinesis, in which case the cell would often pinch off between unsegregated chromosomes. The timing from NEBD to cytokinesis was similar to control cells, suggesting that the defects did not elicit a checkpoint. At higher concentrations of Y-27632, cytokinesis was also inhibited.

Inhibition of Myosin II Disrupts Spindle Assembly in Round Cells

Disruption of myosin II results in cell flattening, which might impede spindle assembly. To circumvent this possibility, we repeated our drug studies in round cells, whose shape was not affected by myosin II disruption. Round B6-8 hybridoma cells were treated with DMSO (Figure 3A), Y-27632 (Figure 3B), or blebbistatin (Figure

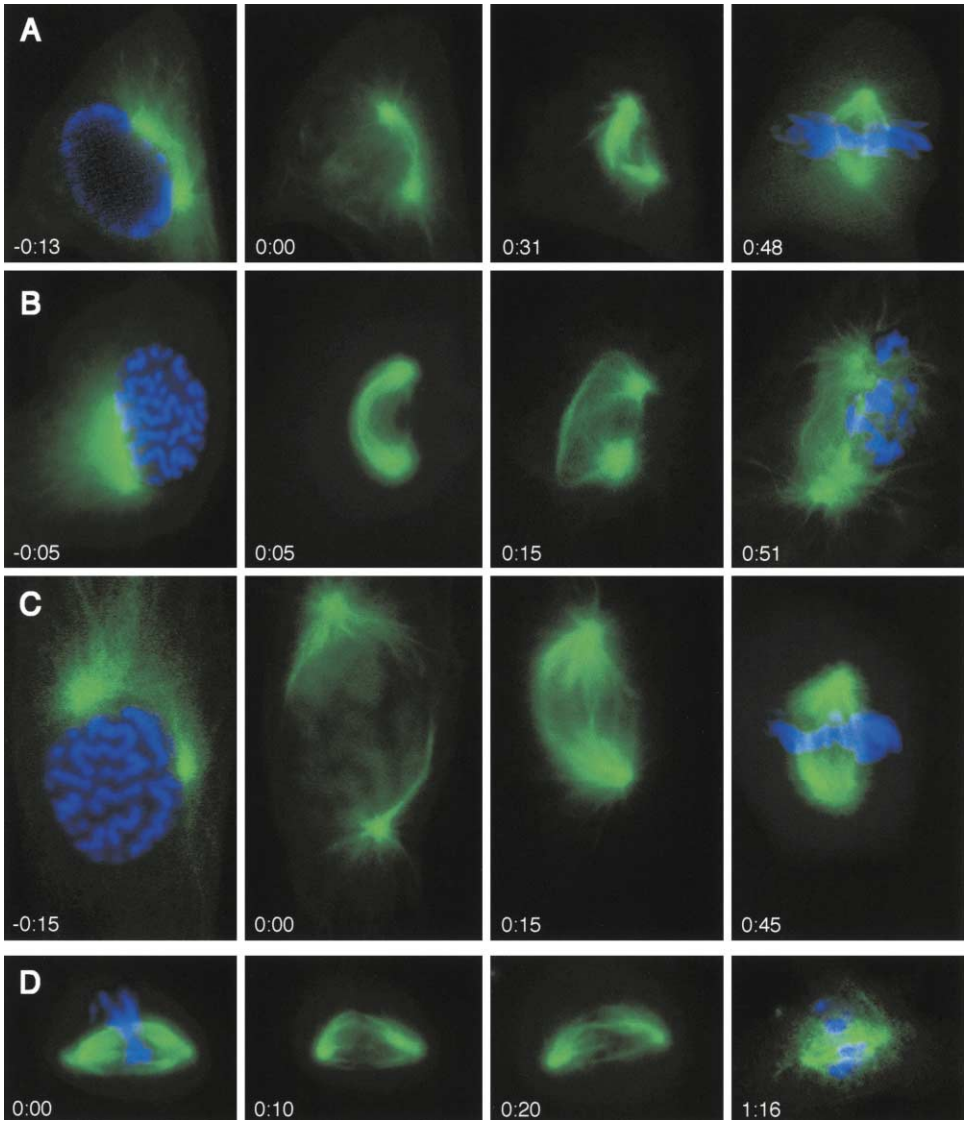

Figure 2. Drug Inhibition of Myosin II Prevents Completion of Centrosome Separation after NEBD

Individual frames from movies show spindle assembly in PtK2 cells expressing GFP-tubulin (green) and Hoechst dye (blue) (A–D). In an untreated cell (A) (see Supplemental Movie S1), the centrosomes migrated around the nuclear envelope until it broke down (0:00). The centrosomes were then pulled further around the condensed chromosomes and the spindle aligned (0:48). In a Y-27632-treated cell (B) (see Supplemental Movie S2), the centrosomes separated along the nuclear envelope until NEBD occurred (0:00), then centrosome migration halted, and the spindle failed to form normally (0:51). In another Y-27632-treated cell (C) (see Supplemental Movie S4), NEBD occurred after completion of centrosome separation around the nuclear envelope (0:00), and the spindle appeared to form normally (0:45). If Y-27632 is added to a spindle after it has assembled (D) (see Supplemental Movie S5), the spindle maintains its morphology; however, it does not enter anaphase or cytokinesis. Thus, myosin II activity is essential for the formation of a spindle after NEBD but not for maintenance of preformed spindle. Time in hr:min.

3C) and fixed and stained for actin, tubulin, and DNA. While the drug treatments had no effect on cell shape (Figures 3B and 3C), they caused more than half of the spindles to form aberrantly (Figure 3D), suggesting that the effects on spindle formation were direct and not secondary to effects on cell shape. Importantly, disruption of myosin II with either drug mainly produced lopsided spindles (Figure 3E), the most common type of defect seen when spindle assembly is disrupted by myosin II inhibition in PtK2 cells (Figures 1B and 1E). The other predominant spindle defect normally seen in PtK2 cells, at poles, is difficult to detect in these round cells, as the condensed chromosomes fill the volume of the cell (see Figure 3A for a normal polarized spindle). Thus, we suspect that the defects scored in Figures 3D and 3E may underestimate the actual numbers of spindle defects produced by myosin II inhibition in round cells.

Inhibition of Myosin II by RNAi Also Disrupts Spindle Assembly

To independently test whether myosin II is required for normal spindle formation, we specifically knocked down

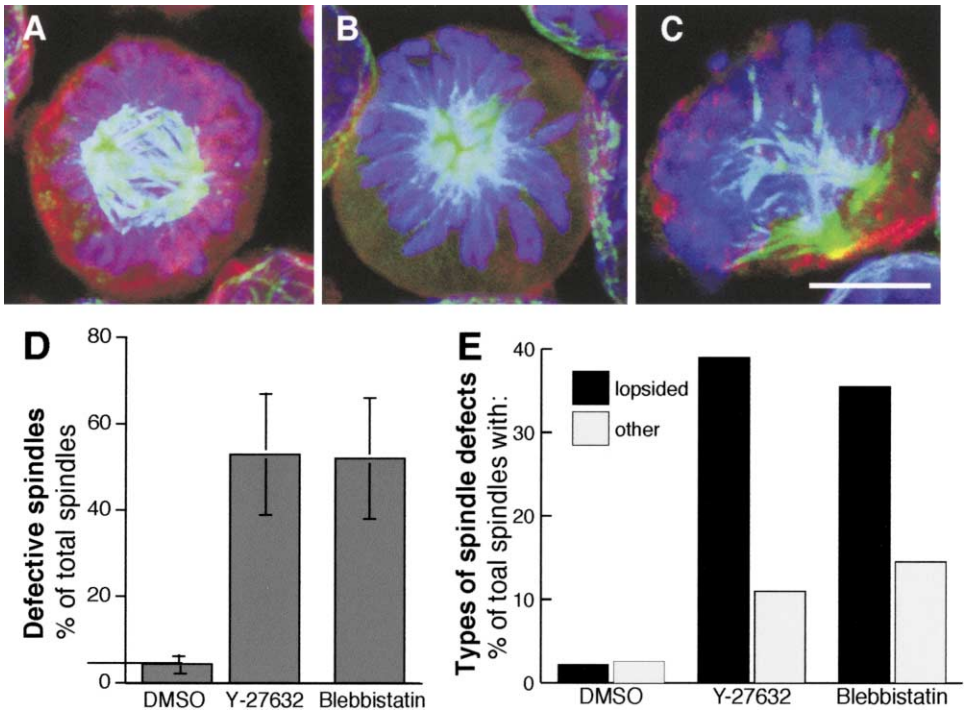

Figure 3. Drug Inhibition of Myosin II Interferes with Normal Spindle Assembly in Round Cells

Confocal projections of B6-8 hybridoma cells treated with 0.1% DMSO (A), 10 μM Y-27632 (B), or 100 μM blebbistatin (C) and immunostained with α-tubulin antibody (turquoise), Hoechst for DNA (blue), and phalloidin for actin (red). Scale bar, 10 μ. The defects in both (B) and (C) show lopsided chromosome spindles, as seen in the flatter PtK2 cells. Because of the angle viewed and the roundness of the cell, the poor separation of the two centrosomes can be seen more clearly in (C) than in (B). Percentage of abnormal spindles from each drug treatment after 4 hr represented as the mean (± SD) of 100 spindles over three experiments (D). As in other cells, lopsided chromosomes are the most common spindle defects seen in round cells (E).

the expression of myosin II using RNAi in the *Drosophila melanogaster* S2R+ cell line. Double-stranded RNAi encoding GFP (control, Figure 4A), myosin II heavy chain (zipper, Figure 4B), or MLC (squash, Figure 4C) was added to the culture medium for 2, 4, 6, 8, or 10 days. The cells were then fixed and stained for actin, tubulin, and DNA. The immunoblot in Figure 4C shows that approximately 96% of cellular myosin II heavy chain was depleted by 6 days of treatment of myosin II heavy chain RNAi. It was also clear that myosin II heavy chain and light chain were depleted by RNAi, as cytokinesis was blocked in these cells compared to the untreated and GFP RNAi-treated control cells (Figure 4E). To avoid scoring aberrant spindle structures that resulted from excess centrosomes due to cytokinesis failure, we scored the spindle defects on day 4 or 6, when the first cytokinesis defects became apparent. We also omitted spindles containing multiple but well-formed asters typically seen in multinucleate cells.

At day 4–6 of RNAi disruption of myosin II heavy chain or light chain, 65%–70% of spindles were defective in morphology (Figure 4E). As with drug disruption of myosin II in hybridoma or PtK2 cells, the most common spindle defect seen with either myosin II heavy or light chain RNAi was lopsided chromosomes (see Figures 4B and 4F). The range of spindle defects was also similar, except that multiple asters were more frequent in cells resulting from myosin II heavy chain RNAi treatment (Figure 4F). This was likely due to the fact that depletion of myosin II, rather than inactivation caused by drug inhibition or depletion of the light chain, structurally compromised the integrity of the cortex (notice decreased cortical actin staining in the cell with multiaster in Figure 4C). We suspect the multiaster defect is due to the ability of microtubules to self organize into asters in mitotic cytoplasm when not constrained by cortical contacts, as seen in in vitro spindle assembly assays using concentrated extracts (Sawin and Mitchison, 1991). Controls cells where no RNAi (data not shown) or GFP RNAi (Figure 4A) was added to S2R+ cells produced normal spindles (Figure 4E), suggesting that the spindle defects were caused from knocking down myosin II specifically.

Crosslinking the Cell Surface with Lectins Also Inhibits Completion of Centrosome Migration

Although myosin II localizes mainly to the cortex during mitosis, some of it also localizes diffusely within the cytoplasm (see Figure 1A). To test whether the spindle defects seen above resulted from inhibiting myosin II within the cortex, we added extracellular tetravalent lectins to inhibit myosin II-dependent movement specifically in the cortex. Wheat germ agglutinin (WGA) and concanavilin A (Con A), when added at high concentrations to the cell medium, bind to cell surface glycoproteins and act to effectively crosslink the cell cortex. These lectins have been shown to block the actin- and myosin II-dependent cortical flow seen in *Xenopus*

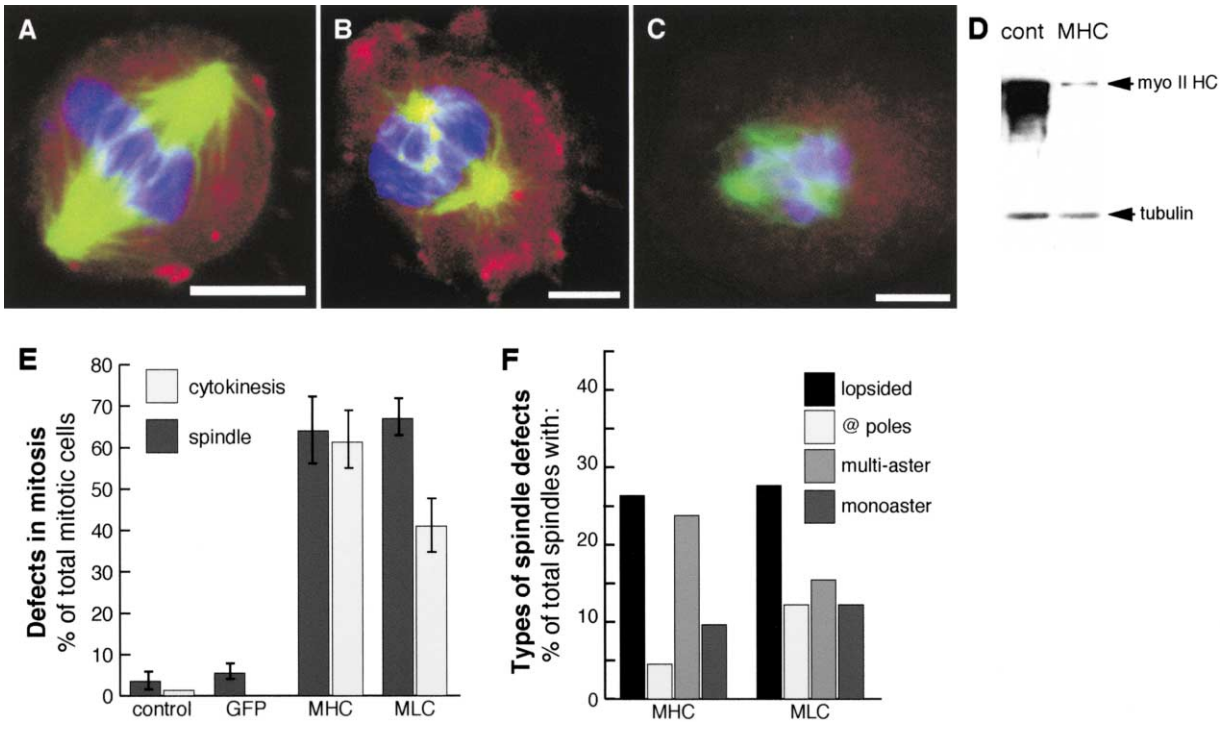

Figure 4. RNAi Depletion of Myosin II Disrupts Spindle Formation in *Drosophila* Cells in Culture

SR2+ cells were treated with dsRNA encoding GFP (A), myosin II light chain (MLC) (B), or myosin II heavy chain (MHC) (C) for 4–6 days and immunostained with antibody to α-tubulin (green), phalloidin for actin (red), and Hoechst for DNA (blue). Scale bar, 5 μm. The most common defects seen were lopsided chromosomes (B) and multiasters (C). Note that with the multiaster defect, the cortex is typically depleted of actin, as in (C). Immunoblot showing MHC is largely depleted after 6 days of RNAi treatment compared to the control lane, where tubulin antibodies are used for loading control (D). Percentage of spindle and cytokinesis defects seen after 4–6 days of RNAi treatment with each dsRNA (E) shown as the mean (± SD) of three experiments from over 150 spindles. RNAi depletion of MHC and MLC causes spindle defects similar to myosin II disruption by drugs (F).

laevis oocytes (Canman and Bement, 1997; Tencer, 1978). Figure 5A and Supplemental Movie S6 show an EGFP-tubulin-expressing PtK2 cell treated with WGA, where NEBD has occurred prior to completion of centrosome migration. As with Y-27632-treated cells, centrosomes do not complete migration around the chromosomes after NEBD but instead stay stuck on one side, producing a "lopsided chromosome" spindle defect. Similarly, the inhibition of cortical movement with lectins only inhibited spindle assembly in cases in which the centrosomes had not completed migration at the time of NEBD. In movies of spindle assembly with WGA, when NEBD occurred prior to completion of centrosome migration, eight out of eight spindles were disrupted, whereas zero out of nine spindles were disrupted when NEBD occurred after centrosome migration was complete.

To quantify the spindle defects resulting from lectin treatments, we analyzed the percentage of spindle defects and the frequency of different types of spindle defects in fixed PtK2 cells pretreated with either WGA or Con A (Figures 5B and 5C). As with myosin II inhibition, approximately 50% of spindles were defective (Figure 5B), and the lopsided chromosome defect was the most common type of defect detected, comprising 33% of all WGA-treated and 41% of all Con A-treated spindles, or greater than 66% of the total spindle defects seen (Figure 5C). That 50%–60% of total spindles were defective when cells were treated with tetravalent lectins is consistent with the analysis of live cells (see above) in which spindle defects only occurred the ~50% of the time that NEBD occurred prior to completion of centrosome migration. Consistent with the idea that the lectins interfered with spindle assembly by crosslinking the cortex, the tetravalent lectins WGA and Con A were more effective at disrupting spindle formation than was the same concentration of succinyl Con A, a divalent lectin that is less efficient at crosslinking the cortex (Figure 5B).

The Cortex Moves in the Direction of Centrosome Migration during Spindle Assembly and Positioning

To examine how cortical myosin II activity might contribute to the movement of centrosomes during spindle assembly, we visualized cortical movement by adding fluorescent latex beads to the surface of PtK2 cells expressing EGFP-tubulin. Fluorescent latex beads have been shown to bind cell surface receptors associated with the underlying cortical actin cytoskeleton during mitosis and have therefore been used to track cortical movement, or flow (Wang et al., 1994). In the control cell in Figure 6A and Supplemental Movie S7, red latex beads on the cell surface moved in the direction of centrosome migration during spindle formation and po-

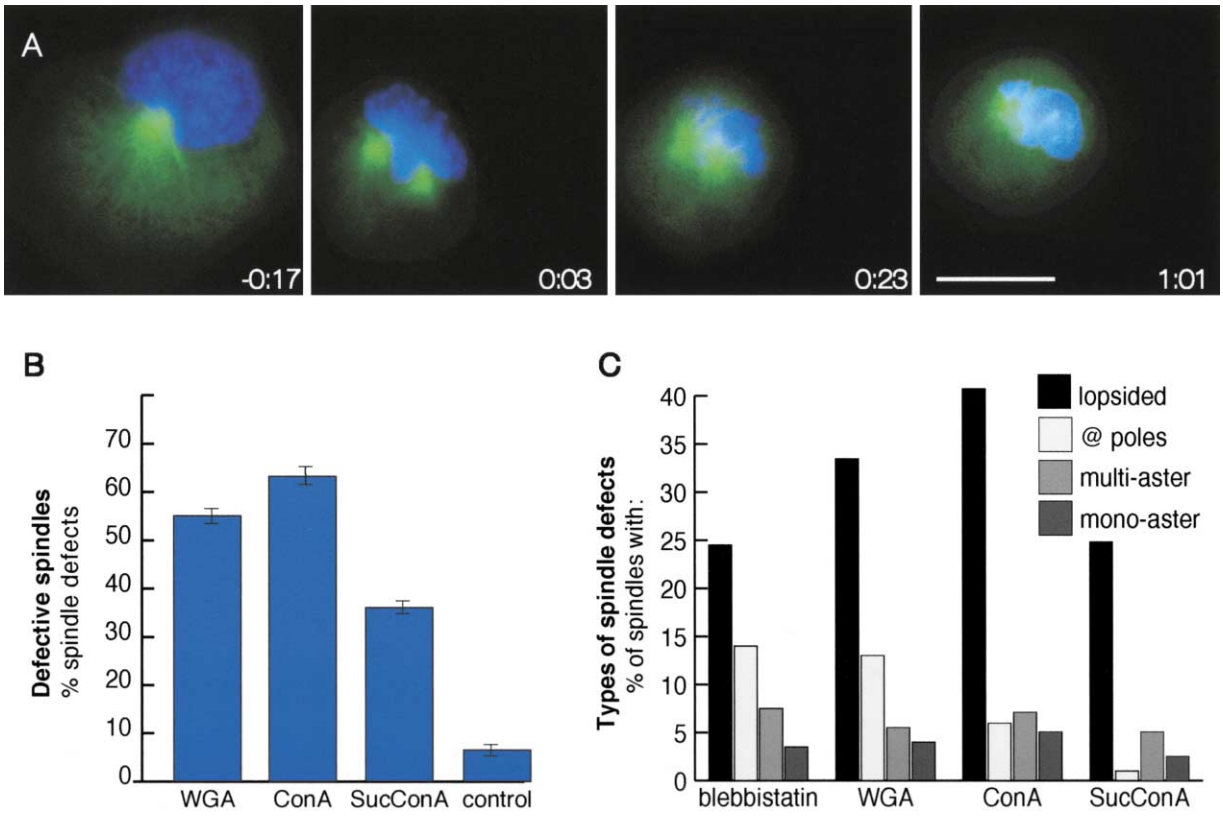

Figure 5. Inhibition of Cortical Flow by Addition of Tetravalent Lectins Inhibits Centrosome Separation around Chromosomes

Stills from Supplemental Movie S6 show defective spindle assembly in the presence of 200 μg/ml WGA (A). Once NEBD occurs at 0:00, centrosomes halt migration around the condensed chromosomes and produce a lopsided chromosome defect (0:20), which is maintained as the chromosomes begin to decondense (1:04). The percentage of spindle defects after addition of the tetravalent lectins WGA and Con A and the divalent lectin Succinyl Con A (B), shown as the mean (± SD) of three experiments from over 400 spindles. As with myosin II inhibition, the most common defect scored with either tetravalent lectin was lopsided chromosomes (C).

sitioning after NEBD. Bead movement is best illustrated by the bead tracks (yellow arrows) made throughout the course of spindle formation. The end points are marked by arrowheads, and the outline of the cell is traced in yellow at the beginning frame of the movie (Figure 6B). Note that the greatest cortical movement is restricted to the middle region of the cell (yellow arrows), where the centrosomes (white arrows) are also moving, and that there is little movement outside of this zone (blue arrows). Movement of the beads along the length of the cell does not reflect a stretching of the cell, as the cell actually contracts slightly over time. Instead, it reflects the movement of the cortex in the direction of centrosome separation and positioning. From the movie (see Supplemental Movie S7), there appear to be two phases of cortical movement: a rapid, early movement perpendicular to the length of the cell that correlates with spindle formation and then a slower movement parallel to the length of the cell that coincides with placement of the spindle within the cell. These two phases of cortical movement are also illustrated in the yellow bead tracks (Figure 6B), which, during spindle assembly, move to the left and up, near the left centrosome, and to the right and down, near the right centrosome. Then, during spindle positioning, all the lower yellow tracks move downward along the length of the cell (Figure 6B). The length of the tracks from the beads and the centrosomes are approximately the same length, suggesting that the rates of movement from the two are also similar.

When myosin II is blocked by addition of Y-27632, centrosome movement after NEBD is blocked, as is movement of the cortex (marked by the red latex beads) (Figure 6C and Supplemental Movie S8). The track marks in Figure 6D show that very little movement of the beads occurs throughout the period filmed, either close (yellow arrows) or distant (blue arrows) to the centrosomes (white arrows).

Kymographs also depict the movement of beads within one xy plane. Here, the position of beads through a given line (represented by hatched lines in Figures 6A [0:00] and 6C [0:00]) is tracked in space and time (Figures 6E and 6F, where distance = x axis, and time = y axis, from top to bottom). Thus, a diagonal line represents movement of a bead or bead cluster, whereas a vertical line represents a static bead. Slower movement produces a diagonal line with a steeper slope, and faster movement produces a shallower slope. Kymographs of the beads on the control cell in Figure 6A show that beads within the middle region near centrosomes migrate outward from the middle of the cell—first rapidly at ~0.6 μm/min for about 20 min during spindle formation and then more slowly at ~0.2 μm/min for about 40

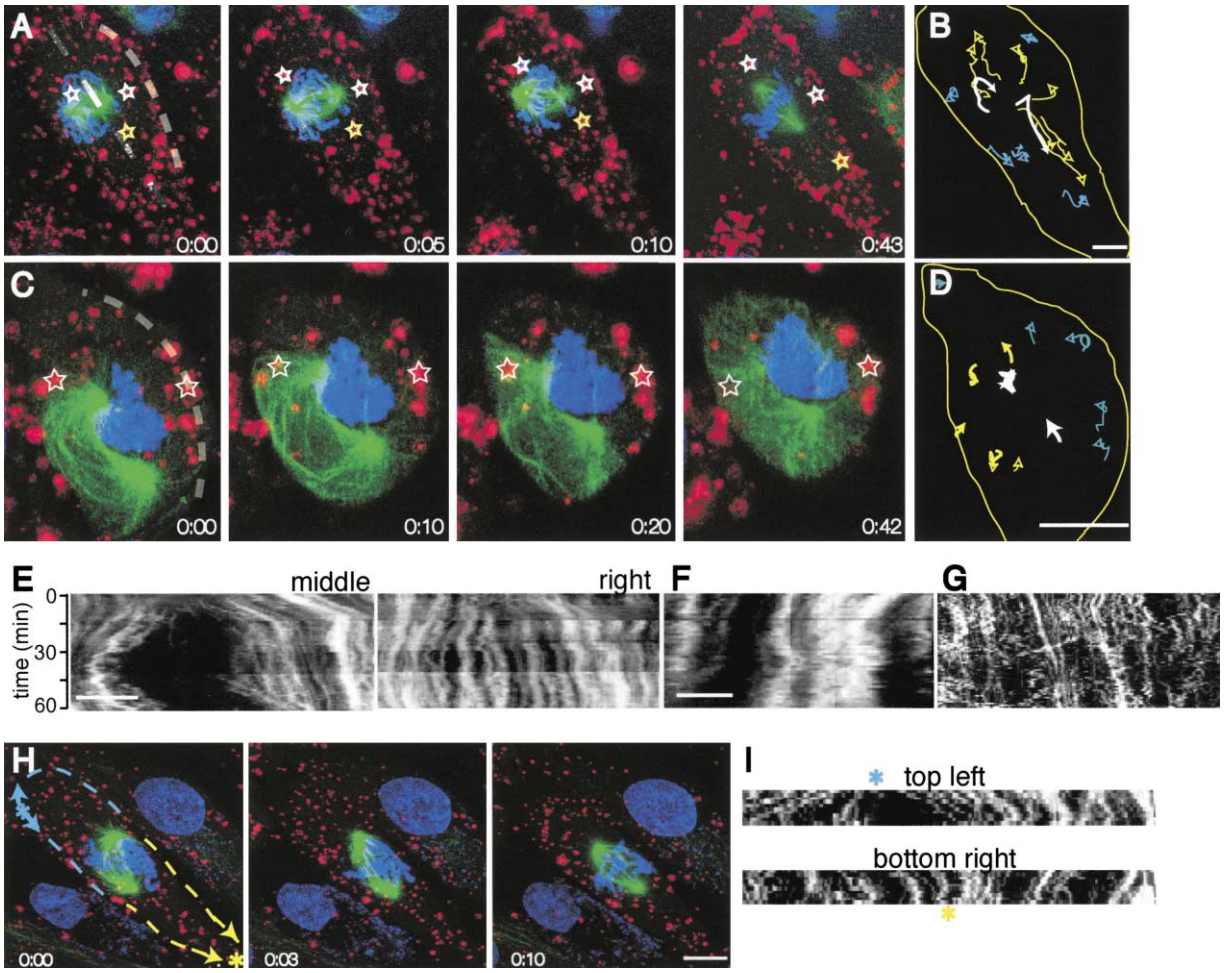

Figure 6. Myosin II-Dependent Cortical Contraction Is Localized during Mitosis and Results in Movement of the Cortex in the Direction of Centrosome Migration

Stills from movies of spindle assembly in PtK2 cells, expressing EGFP-tubulin (green) with Hoechst for chromosome staining (blue) and red fluorescent latex beads added to the cell surface to mark cortical movement (A and C). In the control cell (A and Supplemental Movie S7), red beads migrate in the same direction as centrosomes during spindle assembly ([A], 0:00–0:20) and positioning ([A], 0:20–0:60), where representative beads are marked by white stars (during assembly) and yellow stars (during positioning). Stills from Supplemental Movie S8 of a Y-27632-treated cell show no movement of centrosomes or beads (C) where representative beads are marked by white stars. Tracks made by individual bead (yellow and blue arrows) and centrosome (white arrows) movements in the control (B) and Y-27632-treated cell in (D) have been normalized for cell rounding, where the yellow outline traces the cell at time 0:00. In the control (B), centrosomes (white arrows) move in the same direction and at the same rate (i.e., arrows have similar length) as beads near centrosomes (yellow arrows), whereas beads distant to centrosomes (blue arrows) in control and the beads in the Y-27632-treated cell (D) show little movement. Kymographs (position-time plots) showing the movement of beads on the cells in (A) and (C) ([E] and [F], respectively). Beads near centrosomes (along the dashed line in middle of cell in [A]) move rapidly during spindle assembly (0:00–0:20) and slowly during spindle positioning (0:20–0:60) (E). Reduced bead movement in both the cortex distant to centrosomes in the control cell (right dashed line in [A]) and in a Y-27632-treated cell ([C], dashed line) produce comparatively vertical lines in kymographs ([E] and [F], respectively). A kymograph through a typical interphase cell shows no bead movement (G). Contraction/expansion of cell cortex, marked with beads during spindle assembly after NEBD in a control cell (H and I). Stills of Supplemental Movie S9 indicate the direction of centrosome separation during spindle assembly (H). Kymographs show beads on the side of the cortex nearest separating centrosomes ([H], blue hashed line) move apart ([I], top left), while beads on the other side of the separating centrosomes ([H], yellow hashed line) contract inward ([I], bottom right). Scale bars, 10 μm.

min during subsequent positioning of the spindle within the cell (Figure 6E, middle). By contrast, the kymograph from the top right of the cell, distant to centrosomes, in Figure 6A indicates little movement of beads within this zone. Kymographs of the regions indicated in the myosin II-inhibited cell in Figure 6F (0:00), near centrosomes, with only vertical lines, show no bead movement. By measuring movement of beads using kymographs, we found that in four out of four control movies, bead movement occurred in the same direction and time as centrosome movement, whereas in three out of three movies, when spindle assembly was blocked with Y-27632, bead movement was also blocked. In addition, we found that cortical movement, as measured by bead kymographs, was restricted to mitotic PtK2 cells. In Figure 6G, we show a typical kymograph through the middle of an

interphase PtK2 cell, where vertical lines indicate no bead movement. Findings were similar in five other interphase cells.

Coordinated Cortical Expansion and Contraction Directs Cortical Movement

How could movement of the cortex be regulated? One possibility is that movement occurs only locally at sites near the centrosomes. Another possibility is that the cortex is circumferentially moving. Expansion of the cortex on the side of the cell near centrosomes is driven by contraction on the opposing side. Because Figure 6A shows bead movement on the top of the cell, cortical movement cannot be viewed on the opposing side of the cell that is attached to the glass substrate. Supplemental Movie S9 and representative stills in Figure 6H show cortical movement on both sides of the cell during spindle formation. The bead movement is difficult to detect over the short time sequence (10 min) of Supplemental Movie S9 but, rather, provides a reference to show the direction of centrosome migration as the spindle assembles and for the kymographs. The kymograph in Figure 6I depicting bead movement from the top left region of the cell (indicated by the blue hatched line in frame 0:00 of Figure 6H) shows that the cortex is expanding in the half of the cell encompassing the separating centrosomes (from centrosome to centrosome). By contrast, the kymograph of bead movement from the bottom right half of the cell (indicated by the yellow hatched line) shows that the cortex is contracting on the side opposite to where the centrosomes separate. Coordinate cortical expansion and contraction were seen consistently during spindle assembly after NEBD in three out of three movies where both sides of the cell could be viewed as the spindle formed. These results are consistent with myosin II activity, acting to cause a sink of focused cortical contraction on one side of the cell, which then pulls apart the cortex on the opposing side of cell, nearest to centrosomes. Because the centrosomes are attached to the cortex via astral microtubules, the resulting expansion of the cortex drives centrosome separation.

Discussion

While it was previously established that mitotic spindle assembly depends on microtubules and their associated motor proteins, our findings show that assembly also depends on cortical myosin II. Using several methods to inhibit myosin II and cortical movement, we find that continued separation and positioning of centrosomes around the chromosomes depends on myosin II in the cortex. Cortical myosin II activity drives circumferential movement of the cortex away from attached asters, which acts to separate these asters around the condensed chromosomes. This cortex-dependent movement becomes critical when other mechanisms of separating centrosomes along the nuclear envelope are lost upon NEBD. Because we have seen this dependence in human, rat, and *Drosophila* cell lines, we think that it is likely to be important for all cells in which the nuclear envelope breaks down during mitosis.

Myosin II Inhibition

It is surprising that a requirement for myosin II in spindle formation has not been previously detected. Previous genetic studies showed that myosin II mutations in *S. pombe* (Bezanilla et al., 1997), *D. discoidum* (de Hostos et al., 1993), and *C. elegans* (Shelton et al., 1999) produced only cytokinesis defects. However, the nuclear envelope does not break down during mitosis in *S. pombe* and *D. discoidum*, and it does so only just prior to anaphase in *C. elegans* (Lee et al., 2000). Since the spindle defects we see are dependent on NEBD, we would not expect myosin II mutations to cause spindle defects in any of these organisms. In other multicellular organisms where NEBD occurs prior to metaphase, we would expect about half the cells with myosin II mutations to be able to form normal spindles and then to fail at cytokinesis. The remaining cells would form abnormal spindles, which would then be removed by apoptosis and phagocytosis, making a spindle defect phenotype difficult to score. Indeed, in cells subjected to long-term treatment with myosin II RNAi, we found that few cells survived but that those that did were very large and contained many nuclei and engulfed apoptotic bodies (our unpublished data). Additionally, maternal wild-type protein might confound the analysis of such mutants; the building of new structures such as the cytokinetic ring may require more myosin II than the maintenance of a preformed cell cortex. Thus, embryos with myosin II mutations would most likely display a primarily cytokinesis-defective phenotype.

A directed study of myosin II in single cells used inhibitory antibodies (Kiehart et al., 1982), which inhibited cytokinesis only after 1–2 cell divisions and may inhibit myosin II less effectively in a preformed structure such as the cortex than in an assembling contractile ring. Furthermore, as nuclei were seen to fuse at later times, it is likely that this inhibition eventually blocked mitosis. Although the myosin II inhibitors Y-27632 and blebbistatin are relatively new drugs and have not previously been used in spindle-assembly studies, RNAi depletion confirms that these defects result specifically from myosin II inhibition. Thus, discovery of a new role for myosin in spindle formation has been enabled by new techniques that more rapidly and effectively inhibit myosin II.

Cortical Actin and Myosin II Are Required for Centrosome Separation after NEBD

As shown in the model in Figure 7A, centrosomes can separate along the nuclear envelope in the absence of myosin II activity before NEBD. The cortical-independent centrosome separation along the nuclear envelope presumably relies on dynein and dynactin, which localize to the nuclear envelope prior to NEBD (Busson et al., 1998), as well as on the Eg5/BimC class of kinesins. While the forces required for centrosome migration around the nucleus are not well understood, some evidence for the importance of dynein and dynactin comes from studies in which inhibition of dynein results in monopolar spindles and detachment of the centrosomes from the nuclear membrane (Robinson et al., 1999; Vaisberg et al., 1993). In addition, inhibition of the BimC/Eg5 motors results in monoaster formation and

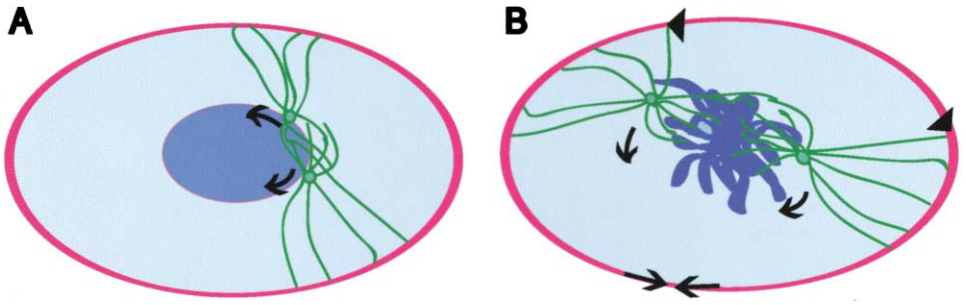

Figure 7. Model for the Role of Myosin II-Dependent Cortical Movement in Aster Separation and Spindle Positioning during Spindle Assembly

Before NEBD, the two asters can separate by moving along the nuclear envelope (A). This movement likely depends on dynein/dynactin complexes at the nuclear envelope and the pushing apart of antiparallel microtubules by Eg5-type motors. Once NEBD occurs, further separation of the asters around the chromosomes and correct spindle placement within the cell require myosin II activity within the cell cortex (B). Localized cortical contraction away from separating asters (indicated by straight black arrows) drives expansion of the cortex nearest asters, which via astral microtubule connections to this expanding cortex acts to separate the asters around the chromosomes (curved black arrows). As microtubule contacts to the cortex are inhibitory to cortical contraction, contraction would be limited near astral microtubules, thereby allowing net expansion of the cortex at this site (arrowheads). Cortical contraction becomes balanced and stops once the number of astral microtubules becomes equally balanced on either side of the cell, which consequently stops migration of asters. Blocking cortical movement still maintains astral microtubule connections to the cortex but prevents aster separation so that spindle assembly typically halts in the lopsided chromosomes position seen in (B).

suggests that these motors contribute to centrosome separation by pushing antiparallel microtubules apart (Kapoor et al., 2000; Sawin et al., 1992).

After NEBD, dynein and Eg5 motors are no longer sufficient for centrosome separation, which now depends upon astral microtubule connections to the cortex (Figure 7B). Although actin and myosin II may also contribute to centrosome separation prior to NEBD, this contribution only becomes apparent after NEBD. It is also possible that at approximately the same time as NEBD occurs, Eg5 motors run out of antiparallel microtubules to push against, an event less obvious than NEBD. In support of this possibility, we find that if we produce monoasters with no nuclear envelope by adding the Eg5 inhibitor monastrol (Kapoor et al., 2000), these monoasters can be rescued only to the lopsided chromosome defect if monastrol is washed out in the presence of a myosin II inhibitor (our unpublished data).

How might cortical actin and myosin II contraction bring about centrosome separation? One possibility is that myosin II directly moves astral microtubules along cortical actin filaments. However, to date there are no clear examples of myosin II motors directly moving microtubules on actin filaments (Rodriguez et al., 2003). An alternative model is that astral microtubules bind to a moving cell cortex (Figure 7B). This model is supported by our findings that cell surface bound fluorescent latex beads that mark the cell cortex move in the direction of the separating centrosomes. Furthermore, myosin II inhibitors or tetravalent lectins that block this cortical movement also block centrosome separation.

From previous studies on directed cortical movement, termed cortical flow, we predict that myosin II-based contraction acts to pull astral microtubules in the plane of the cortex toward the site of contraction (Figure 7B) (Hird and White, 1993; Mandato and Bement, 2003). This type of mechanism has been shown to cause the directed movement of microtubules along cortical actin filaments during wound healing experiments in *Xenopus* oocytes (Mandato and Bement, 2003). In these studies, myosin II-based purse-string contraction at the wound site acts to pull in cortical actin filaments as well as the microtubules that are attached to the actin filaments. In our studies using beads to visualize the location and direction of cortical movement during spindle assembly, contraction of the cortex on the side of the cell opposite to where centrosomes are separating causes a coordinate expansion of the cortex on the side where centrosomes are migrating apart (Figure 7B).

Although we know that the cortex moves in conjunction with centrosome separation and that this separation is dependent on cortical movement, we do not yet understand what regulates the direction of cortical movement or what stops this movement once centrosome migration and positioning are complete. One attractive model is that the astral microtubules might be responsible for this regulation. Microtubule binding to the cortex has been shown to decrease cortical flow rates (Benink et al., 2000; Canman and Bement, 1997; Hird and White, 1993). Thus, in our model (Figure 7B), astral microtubule connections to the cortex would locally dampen myosin II activity and thereby cortical contraction at that location, whereas contraction elsewhere would be unaffected. Hence, localized cortical contraction distal to the asters (inward arrows) would drag astral microtubules (arrowheads) toward the site of contraction (inward arrows) and thereby separate centrosomes around the condensed chromosomes (curved arrows). Drag force would cause compensatory expansion of the cortex proximal to the asters (arrowheads), as we have observed. As cortical contraction is suppressed near astral microtubules and enhanced away from them, the circumferential contractile force of the cortex would be weak between the separating asters and strong away from them (arrows). When the spindle poles reach the opposite ends of the cell, astral microtubule contacts to the cortex would become equal and opposite so that the cortical contraction would be balanced, thereby stopping further centrosomal migration. As suggested previously, this same mechanism may also act later dur-

ing cytokinesis to position actin and myosin II contraction between the spindle poles, where fewer microtubules contact the cortex (Hird and White, 1993; Mandato et al., 2000). While regulation of cortical movement requires further investigation, our results underscore the importance of cortical myosin II forces for assembling a spindle and provide a new mechanism that accounts for how this newly forming spindle becomes correctly positioned within the framework of a cell.

Experimental Procedures

Cell Culture

PtK2 cells were cultured in DMEM and B6-8 hybridoma cells in RPMI medium with 10% fetal bovine serum and 100 μg/ml penicillin/streptomycin (all from GIBCO BRL) at 5% CO_2 and 37°C. *Drosophila* S2R+ cells were cultured in 40% S2 and 60% SFM medium with 10% fetal bovine serum and 100 μg/ml penicillin/streptomycin (all, GIBCO/BRL) at 25°C.

Transfections

An EGFP-tubulin plasmid (Clontech) was transfected into PtK2 cells using a Lipofectamine Plus Kit (GIBCO BRL) and selected using 100 μg/ml G418 (GIBCO BRL).

Cell Staining

Cells were fixed with 100% methanol at −20°C for 2 min, rinsed three times in phosphate buffered saline (PBS), permeabilized for 5 min with PBS containing 0.5% Triton X-100, and blocked in AbDil (PBS with 0.1% Triton X-100 and 2% bovine serum albumin). Cells were stained with 1:100 anti-tubulin ascites (Sigma, DM1α), 1 μg/ml Hoechst (Sigma), and either 1:50 nonmuscle myosin II polyclonal antibody (Biogenesis) or 1:200 actin polyclonal antibody (Sigma, A2066).

RNAi Treatment

RNAi depletion of GFP, MHC, and MLC was carried out according to the methods in Kiger et al. (2003). For protein detection on immunoblots, approximately 5 μg of control or 6 day RNAi-depleted MHC lysates were loaded on gels and probed with antibodies to *D. melanogaster* myosin II heavy chain (1:5000, a generous gift from Christine Field) and to tubulin (1:1000 DM1α [Sigma]).

Drug Treatment

Cells were treated with 100 μM blebbistatin (a generous gift from Aaron Straight and Timothy Mitchison), 5 μM Latrunculin A (Calbiochem), and 10 μM Y-27632 (Tocris) for the times indicated.

Image and Movie Acquisition

Fluorescence micrographs were obtained using a Nikon Eclipse e800 microscope and captured using a SynSys cooled charge coupled device (CCD) camera (Roper Scientific). Time-lapse movies were made using an Axiovert microscope (Zeiss) and captured using a Micromax CCD camera (Roper Scientific). Metamorph software (Universal Imaging) was used to control the camera and to process images. Confocal micrographs were obtained using a Bio-Rad multiphoton and Nikon microscope, and Z sections were reconstructed using Confocal Assistant (BioRad). All images were processed further using Adobe Photoshop and Illustrator.

Latex Bead Movies

A coverslip of PtK2 cells expressing EGFP-tubulin was briefly washed with PBS and incubated with a mixture of sonicated red fluorescent latex beads (50 μl of 1 μ red fluorescent latex beads [Sigma] in 400 μl 10mg/ml BSA in PBS) for 2 min and washed twice with chamber medium (1:1 D-MEM:F-12 medium without phenol red and HEPES buffered + 10% fetal calf serum + 100 μg/ml penicillin/streptomycin [all from GIBCO BRL] + 1 μg/ml Hoechst 33342). The cover slip was inverted on a glass slide in chamber medium with or without 10 μM Y-27632 using a silicone fitting (Molecular Probes), and red, green, and blue channels were filmed on three separate Z planes approximately 1–1.5 μm apart every minute on a Nikon microscope using a Bio-Rad multiphoton confocal. Tracking of beads and kymograph analysis were done using Metamorph software (Universal Imaging).

Acknowledgments

We thank Martin Raff, as always, for his generous support and lively discussions about the work and manuscript. We also thank Timothy Mitchison for helpful discussions about experiments and the manuscript and (also Aaron Straight) for generously contributing blebbistatin. We thank Veronica Dominguez for help with RNAi preparation; Christine Field for *Drosophila* myosin II antibody; and James Blyth, Helen Dawe, Alison Lloyd, and Mike Redd for comments on the manuscript. This work was supported by an American Cancer Society postdoctoral fellowship, a Cancer Research UK project grant, and a BBSRC project grant to J.R.; by Royal Society University Research Fellowships to both B.B. and L.P.C.; and by a Wellcome Trust project grant (to L.P.C.). J.R. wishes to dedicate this work in loving memory to Frances Turner—my love is with you always.

Received: May 27, 2003
Revised: February 25, 2004
Accepted: February 25, 2004
Published: April 29, 2004

References

Benink, H.A., Mandato, C.A., and Bement, W.M. (2000). Analysis of cortical flow models in vivo. Mol. Biol. Cell *11*, 2553–2563.

Bezanilla, M., Forsburg, S.L., and Pollard, T.D. (1997). Identification of a second myosin-II in Schizosaccharomyces pombe: Myp2p is conditionally required for cytokinesis. Mol. Biol. Cell *8*, 2693–2705.

Busson, S., Dujardin, D., Moreau, A., Dompierre, J., and De Mey, J.R. (1998). Dynein and dynactin are localized to astral microtubules and at cortical sites in mitotic epithelial cells. Curr. Biol. *8*, 541–544.

Canman, J.C., and Bement, W.M. (1997). Microtubules suppress actomyosin-based cortical flow in Xenopus oocytes. J. Cell Sci. *110*, 1907–1917.

de Hostos, E.L., Rehfuess, C., Bradtke, B., Waddell, D.R., Albrecht, R., Murphy, J., and Gerisch, G. (1993). Dictyostelium mutants lacking the cytoskeletal protein coronin are defective in cytokinesis and cell motility. J. Cell Biol. *120*, 163–173.

Hird, S.N., and White, J.G. (1993). Cortical and cytoplasmic flow polarity in early embryonic cells of Caenorhabditis elegans. J. Cell Biol. *121*, 1343–1355.

Kapoor, T.M., Mayer, T.U., Coughlin, M.L., and Mitchison, T.J. (2000). Probing spindle assembly mechanisms with monastrol, a small molecule inhibitor of the mitotic kinesin, Eg5. J. Cell Biol. *150*, 975–988.

Kiehart, D.P., Mabuchi, I., and Inoue, S. (1982). Evidence that myosin does not contribute to force production in chromosome movement. J. Cell Biol. *94*, 165–178.

Kiger, A., Baum, B., Jones, S., Jones, M., Coulson, A., Echeverri, C., and Perrimon, N. (2003). A functional genomic analysis of cell morphology using RNA interference. J. Biol. *2*, 27.

Komatsu, S., Yano, T., Shibata, M., Tuft, R.A., and Ikebe, M. (2000). Effects of the regulatory light chain phosphorylation of myosin II on mitosis and cytokinesis of mammalian cells. J. Biol. Chem. *275*, 34512–34520.

Lee, K.K., Gruenbaum, Y., Spann, P., Liu, J., and Wilson, K.L. (2000). C. elegans nuclear envelope proteins emerin, MAN1, lamin, and nucleoporins reveal unique timing of nuclear envelope breakdown during mitosis. Mol. Biol. Cell *11*, 3089–3099.

Mandato, C.A., and Bement, W.M. (2003). Actomyosin transports microtubules and microtubules control actomyosin recruitment during Xenopus oocyte wound healing. Curr. Biol. *13*, 1096–1105.

Mandato, C.A., Benink, H.A., and Bement, W.M. (2000). Microtubule-actomyosin interactions in cortical flow and cytokinesis. Cell Motil. Cytoskeleton *45*, 87–92.

Meeusen, R.L., Bennett, J., and Cande, W.Z. (1980). Effect of mi-

croinjected N-ethylmaleimide-modified heavy meromyosin on cell division in amphibian eggs. J. Cell Biol. *86*, 858–865.

Rattner, J.B., and Berns, M.W. (1976). Centriole behavior in early mitosis of rat kangaroo cells (PTK2). Chromosoma *54*, 387–395.

Robinson, J.T., Wojcik, E.J., Sanders, M.A., McGrail, M., and Hays, T.S. (1999). Cytoplasmic dynein is required for the nuclear attachment and migration of centrosomes during mitosis in Drosophila. J. Cell Biol. *146*, 597–608.

Rodriguez, O.C., Schaefer, A.W., Mandato, C.A., Forscher, P., Bement, W.M., and Waterman-Storer, C.M. (2003). Conserved microtubule-actin interactions in cell movement and morphogenesis. Nat. Cell Biol. *5*, 599–609.

Sawin, K.E., and Mitchison, T.J. (1991). Mitotic spindle assembly by two different pathways in vitro. J. Cell Biol. *112*, 925–940.

Sawin, K.E., LeGuellec, K., Philippe, M., and Mitchison, T.J. (1992). Mitotic spindle organization by a plus-end-directed microtubule motor. Nature *359*, 540–543.

Shelton, C.A., Carter, J.C., Ellis, G.C., and Bowerman, B. (1999). The nonmuscle myosin regulatory light chain gene mlc-4 is required for cytokinesis, anterior-posterior polarity, and body morphology during Caenorhabditis elegans embryogenesis. J. Cell Biol. *146*, 439–451.

Silverman-Gavrila, R.V., and Forer, A. (2001). Effects of anti-myosin drugs on anaphase chromosome movement and cytokinesis in crane-fly primary spermatocytes. Cell Motil. Cytoskeleton *50*, 180–197.

Somma, M.P., Fasulo, B., Cenci, G., Cundari, E., and Gatti, M. (2002). Molecular dissection of cytokinesis by RNA interference in Drosophila cultured cells. Mol. Biol. Cell *13*, 2448–2460.

Straight, A.F., Cheung, A., Limouze, J., Chen, I., Westwood, N.J., Sellers, J.R., and Mitchison, T.J. (2003). Dissecting temporal and spatial control of cytokinesis with a myosin II inhibitor. Science *299*, 1743–1747.

Tencer, R. (1978). Transmembrane effects of lectins. I. Effects of wheat germ agglutinin and soybean agglutinin on furrow formation and cortical wound healing in Xenopus laevis eggs. Exp. Cell Res. *116*, 253–260.

Vaisberg, E.A., Koonce, M.P., and McIntosh, J.R. (1993). Cytoplasmic dynein plays a role in mammalian mitotic spindle formation. J. Cell Biol. *123*, 849–858.

Wang, Y.L., Silverman, J.D., and Cao, L.G. (1994). Single particle tracking of surface receptor movement during cell division. J. Cell Biol. *127*, 963–971.

Whitehead, C.M., Winkfein, R.J., and Rattner, J.B. (1996). The relationship of HsEg5 and the actin cytoskeleton to centrosome separation. Cell Motil. Cytoskeleton *35*, 298–308.